Optimization of Process Parameters of Wet-Spun Solid PVDF fibers for Maximizing the Tensile Strength and Applied Force at Break and Minimizing the Elongation at Break using the Taguchi Method

Mevlut Tascan, PhD

Zirve University, Gaziantep TURKEY

Correspondence to:
Mevlut Tascan email: mevlut.tascan@zirve.edu.tr

ABSTRACT

PVDF polymer is well known with its high strength, toughness and piezoelectric properties. It is commonly used in film form for sensor applications, mechanical actuators, energy harvesters, artificial muscles, and membranes. PVDF polymer is also used as hollow fiber membranes in filtration applications, such as nanofiber-web produced using electrospinning and as solid PVDF fiber produced using melt spinning for research purposes. According to a literature study, research on PVDF solid fiber production using wet spinning is limited.

This article is about the optimization of the process parameters of wet-spun solid PVDF fibers for maximizing the tensile strength and applied force at break and minimizing the elongation at break using the Taguchi Method. According to the results, the highest applied force at break was achieved when PVDF fiber made from the process parameters of 12 rpm pump speed, 1.5 mm spinneret diameter, 1.0 draw ratio, and 40°C draw temperature. The highest tensile strength was achieved when PVDF fiber was made from the process parameters of 8 rpm pump speed, 1mm spinneret diameter, 2.0 draw ratio, and 40°C draw temperature. The minimum elongation at break was achieved when PVDF fiber was made from the process parameters of 4 rpm pump speed, 1.5 mm spinneret diameter, 2.0 draw ratio, and 25°C draw temperature. These results may prove that process parameters could be used for the further production of the PVDF fibers. Additionally, the Taguchi method was found to be reliable for optimizing the wet spinning of PVDF fibers.

INTRODUCTION

Poly vinylidene fluoride (PVDF) is known for its good piezoelectric properties, which means PVDF has the ability to convert mechanical energy into electrical energy. It has low cost, highly flexibility, and biocompatibility. The piezoelectric property of PVDF is extensively used in its film form for different applications such as strain sensors, mechanical actuators, energy harvesters, and artificial muscles. [1–5]

Among wet spinning applications, PVDF fibers are produced by the wet spinning process for mesh applications and the produced PVDF fiber is in hollow form. Solid PVDF fiber production using wet spinning was not found in the literature. [6–8]

PVDF polymer has three phases: α-phase, β-phase, and γ-phase as shown in *Figure 1*. The preferred formation of PVDF polymer is α-phase because it is produced at the higher crystallization rate and at higher temperatures (110–150°C). On the other hand, β-phase PVDF polymer crystallizes below 80°C. During melt spinning, crystallized PVDF would be in α-phase because the polymer processing temperatures are more than 150°C. After fiber production using melt spinning, the β-phase of PVDF may be produced by mechanical deformation such as uniaxial stretching. The reason is that during melt spinning, additional drawing under high voltage should be done to change the crystalline phase formation of PVDF from α-phase to β-phase. α-phase PVDF polymers or fibers do not have the ability to generate electricity under stress. To have piezoelectric activity, PVDF polymer should be in β-phase because the fluorine (-) and hydrogen (+) atoms are on the opposite sides of the molecule and therefore polarity is created. β-phase PVDF may be produced when the process temperature during the crystallization of PVDF is less than 80°C. [11, 12]

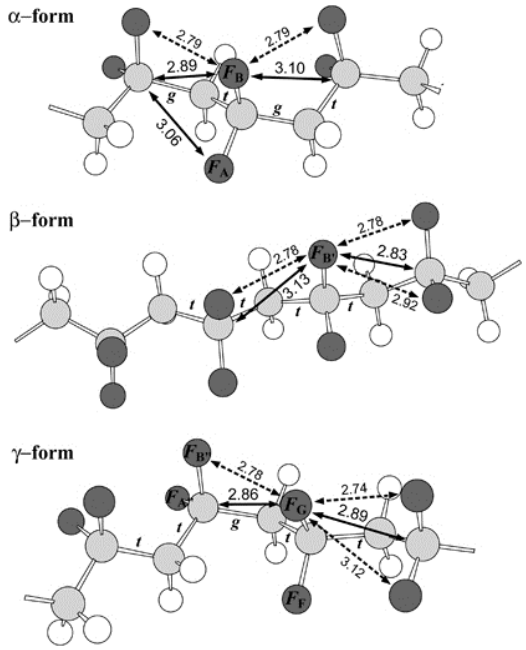

FIGURE 1. Typical phases of PVDF polymer. [9]

Since β-type PVDF polymer production is difficult and additional process steps are needed for melt spinning, wet spinning could be selected to produce PVDF fibers because the temperature is not a major problem for fiber production. The main difference between the melt-spun fiber and wet-spun fiber is that wet-spun fiber has porous formation. The pores in the fiber may affect the piezoelectric property of PVDF fiber. Preliminary results that were done on wet-spun β-type PVDF fibers show higher voltage outputs generated from the fiber. The results also show that it is valuable to optimize the process parameters in wet spinning of PVDF fibers.

The wet spinning process is a conventional process that has been used in industry for more than 70 years and is well known by fiber producers and academicians. *Figure 2* shows a typical wet spinning process. First step involve dissolving PVDF polymer should by a solvent. The PVDF solution is fed to the pump (2) and then to the spinneret (3) in the first bath (5). After the spinneret, the PVDF solution meets with water, which removes the dimethylacetamide (DMA) from the PVDF solution in the first bath, and the PVDF polymer solidifies as fiber. After the first spinning bath, pre-solidified monofilament is wound to the first roller (7) and first drawing occurs because of the speed ratio between the feeding pump speed and the first roller speed.

First drafting of PVDF fiber affects the crystallization structure of the fiber. Then, the fiber is exposed to a second bath (6) for a better solidification, and a second drafting occurs between first and the second rollers (9). The second drawing mostly solidifies the fiber and affects its molecular orientation. If needed, hot air drafting (10) and/or drying can be applied to produce wet-spun fiber prior to winding. The PVDF fiber is then packaged using a bobbin winder (11).

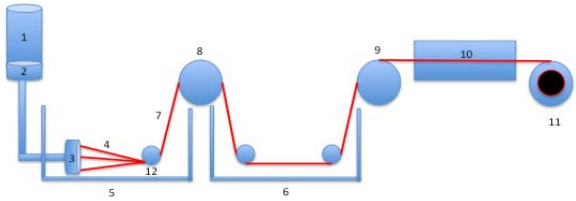

FIGURE 2. Typical Wet-Spinning Set-up (1) Feeding Tank, (2) Pump, (3) Spinneret, (4) Fiber, (5) First Bath, (6) Second Bath, (7) Yarn, (8) First Roller, (9) Second Roller, (10) Air Drawing, (11) Bobbin Winder.

In this research, the Taguchi method was used as the statistical approach. This method is used to establish the minimum set of parameter-level combinations of experiments to optimize product qualities and identifies significant contributions of parameters to the qualities. It has been widely used in recent engineering statistics. [13-16, 19, 20]

The Taguchi method differs from the classical methods by using orthogonal arrays. Orthogonal arrays reduce the number of samples and result in easy to handle experimental designs. In addition, Taguchi methods use different types of signal to noise ratios (S/N ratio) to measure variability around the target performance. [19-20]

The Taguchi method is done by using the following steps for experimental process optimization:

- Process parameters are chosen.
- The number of levels on each process parameter is decided.
- Combined effects of two or more parameters are taken into account.
- Orthogonal arrays are determined based on the number of parameters and parameter levels.
- Selected samples from orthogonal arrays are produced and the property is measured.
- Performance statistics are taken.
- The best option of the levels from the parameters is calculated.

- The best sample is produced and the calculation is verified by measuring the property of the produced sample.
- If the property values are in the calculated tolerance, then the optimization process is finished. If not, then the combined effects of two or more parameters are analyzed.

Table I shows the typical L_9 orthogonal array in the Taguchi method. In this array, four different parameters are selected and each parameter has three levels.

TABLE I. L_9 Orthogonal array in Taguchi Method.

Experiment	P1	P2	P3	P4
1	1	1	1	1
2	1	2	2	2
3	1	3	3	3
4	2	1	2	3
5	2	2	3	1
6	2	3	1	2
7	3	1	3	2
8	3	2	1	3
9	3	3	2	1

P1, P2, P3, P4 are the parameters; 1, 2, 3 are the levels of the parameters.

The objective of this research was to optimize the process parameters of wet-spun solid PVDF fibers for maximizing the tensile strength and minimizing the elongation at break using the Taguchi Method.

MATERIALS AND METHODS

Materials

Kynar Type 740 PVDF polymer from Arkema Chemical Company was used for the PVDF fiber production using the wet spinning process. PVDF polymer was dissolved using DMA with mechanical mixing for 3 hours at 60°C. PVDF amount in the solution was chosen as 20% w/w. The polymer solution temperature during wet spinning was chosen as 25°C. All the PVDF samples were produced using the wet spinning unit located at the Zirve University Fiber Production Center. A total of 9 samples were produced using wet-jet wet spinning process whereby the dissolved PVDF polymer directly met with water that removed the DMA solvent and solidified the PVDF fiber. The spinnerets used in this research were one-holed, thus the resulting samples were all monofilaments.

PVDF samples were drawn only at the second drawing region between the first and the second roller during wet spinning. The PVDF fibers were not drafted in the first drafting region, and hot air drawing and drying steps were not used (10). Four process parameters were selected in three levels of each for the optimization of PVDF monofilament production: pump speed (4, 8, and 12rpm), draw ratio at the second drafting region (1, 1.5, and 2.0), draw temperature at the second drafting region (25°C, 40°C, and 55°C), and the spinneret hole diameter (1, 1.3, and 1.5mm). All the process parameters for the samples are shown in *Table II*.

TABLE II. Wet Spinning Process Parameters that are used to produce PVDF Fiber Samples.

Sample ID	Pump Speed (rpm)	Spinneret Diameter (mm)	Drawing Ratio	Drawing Temperature (°C)
1	4	1.5	1	25
2	4	1	1.5	40
3	4	1.3	2	55
4	8	1.5	1.5	55
5	8	1	2	25
6	8	1.3	1	40
7	12	1.5	2	40
8	12	1	1	55
9	12	1.3	1.5	25

The temperature of the first bath was chosen as 25°C for all fiber productions, and fibers were not drafted in this region. After producing all the samples, PVDF fibers were put into the fresh water for a day to make sure that all the solvent was released from the fiber. After that, fibers were dried for a day at 25°C room temperature and 50% humidity.

Methods

The linear densities (tex) of the fibers were measured by weighing 1m of fibers with ten measurements on each sample. The average of these ten measurements was taken as linear density results. Applied force at break, tensile strength, and elongation at break of were measured according to the ASTM D-3822 method using an INSTRON 5440 test device. A 10cm-fiber length was used for strength and elongation measurements. All other parameters were selected based on the standards.

The SEM pictures were made at the University – Industry – Government Association of Improvement, Application and Research Center in Kahramanmaras Sutcu Imam University using a ZEISS EVO LS10 model SEM device. Before the SEM measurements, samples were coated with gold using a Cressington Sputter 108 Auto coater.

The Taguchi method was applied to the data obtained based on the orthogonal array technique to determine the optimum parameters for maximum tensile strength, maximum applied force at break, and

minimum elongation at break. Therefore, rather than producing 3^4 (81) different fiber samples, production of only 9 samples were sufficient for the optimization study as shown in *Table II.*

The order of experiments was obtained by inserting parameters into columns of the orthogonal array, L_9 (3^4), but it was randomly made to avoid noise sources, which were not considered initially and, could take place during an experiment and affect the results in a negative way. The performance characteristics were chosen as the optimization criteria. Three categories of performance characteristics are known in the Taguchi method, namely the larger-the better, the smaller-the better, and the nominal-the better. These performance characteristics were evaluated by using Eq. (1-3).

$$\text{Larger: } S/N = -10\log_{10}\left(\frac{1}{n}\sum_{i=1}^{n}\frac{1}{Y_i^2}\right) \quad (1)$$

$$\text{Smaller: } S/N = -10\log_{10}\left(\frac{1}{n}\sum_{i=1}^{n}Y_i^2\right) \quad (2)$$

$$\text{Nominal: } S/N = -10\log_{10}\left(\frac{1}{n}\sum_{i=1}^{n}(Y_i - Y_0)^2\right) \quad (3)$$

where S/N are performance statistics, defined as the signal to noise ratio (S/N unit: dB); n is the number of repetitions for experimental combination; and Y_i is a performance value of the i*th* experiment and Y_o nominal value desired.

The experiments were conducted with three replications for the optimization. The average results of these replications for each test are shown in *Table III*. Since it was aimed to minimize the coefficient of variation, S/N values were calculated based on the quality characteristic of "the larger the better" for force and tensile strength using Eq. (1) and "the smaller the better" for the elongation. The levels of each parameter, which maximize the S/N were taken as optimum for the force and tensile strength and the levels of each parameter that minimize the S/N were taken as optimum for the elongation.

In the Taguchi Method, the experiment corresponding to the optimum working conditions may not be performed during experiments. In such cases the performance value corresponding to optimum working conditions can be predicted by utilizing the balanced characteristic of the orthogonal array using Eq. (4).

$$Y_i = \mu + X_i + e_i \quad (4)$$

where μ is the overall mean of performance value; X_i is the fixed effect of the parameter level combination used in i*th* experiment; and e_i is the random error in i*th* experiment.

Because Eq. (4) is a point of estimation, which is calculated by using experimental data to determine whether the results of the confirmation experiments are meaningful or not, the confidence interval must be evaluated. The confidence interval at a chosen error level may be calculated using Eq. (5):

$$CI = \mu \pm \sqrt{F(1, n_2) x V_e / N_e} \quad (5)$$

where μ is an average expected performance statistic at optimum conditions; F (1, n_2) is an F value from the F table from any statistical book at the required confidence level and at DF 1 and error DF n_2; V_e is a variance of error term (from the ANOVA table); N_e is an effective number of replications; and

$$N = \frac{\text{Total number of results (or number of } S/N \text{ ratios)}}{\text{DF of mean (= 1 always)} + \text{DF of all factors included in the estimate of the mean}}$$

RESULTS AND DISCUSSION

Fiber process parameters and their levels were considered to be the best fiber properties for piezoelectrical applications of PVDF fibers. All PVDF fibers, produced for this research, have rounded-rectangular shape as shown in *Figure 3.* Spinneret hole shape was chosen as round but the resulting fiber became rounded rectangular. Since the PVDF fibers are used for their piezoelectric properties and the intention for this research was to produce the fibers for piezoelectric use, rounded rectangular shape was chosen because it has flat ends on both sides, so the potential difference that will be generated from these fibers would be high because of more molecules being reached to get the total value. Having round holes in the spinneret, a spinneret-hole diameter as high as 1mm, and a pump speed slower results in a rounded rectangular shape. This shape will happen after drawing and drying. Therefore, the porosity will also be low because of the collapsing of the fibers after drawing.

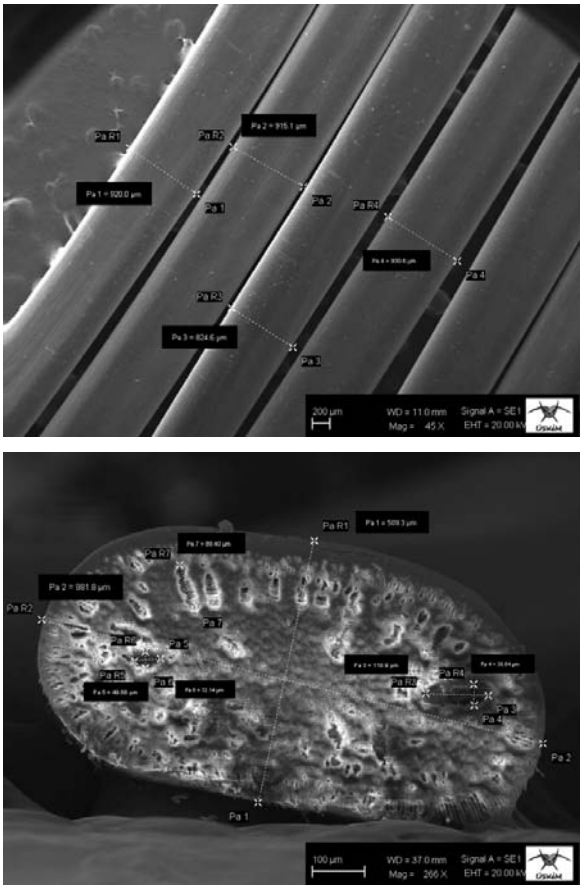

FIGURE 3. Produced PVDF Wet-Spun Fiber.

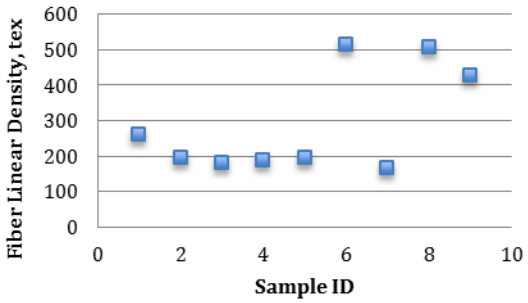

FIGURE 4. Fiber linear density values for each produced PVDF fiber sample.

Linear densities of PVDF samples are shown in *Figure 4*. When 4 rpm pump speed was used, regardless of the spinneret diameter, linear density values were lower at around 200tex. When 8 rpm pump speed (feeding speed) was used, then the drawing ratio affected the tex values. At draw ratios of 1.5 and 2.0, the tex value was again around the 200 tex level. Linear density values increase when no drawing is applied. At the feeding speed of 12 rpm, the values were around 450-500 tex with lower drawing. These results show that, 4 rpm pump speed is very low compared to the spinneret diameter of the monofilament, so the drawing ratio does not affect the fiber linear density. But when the feeding speed is 8 rpm and more, the draw ratio matters; thus, the feeding speed is compatible with the spinneret diameter.

TABLE III. Strength and Elongation Results of PVDF Fibers.

Sample ID	Applied Force at Break (cN)	Tensile Strength (cN/tex)	Elongation at Break (%)
1	139	0.53	18.5
2	170	0.86	23.2
3	171	0.94	12.7
4	167	0.89	25.1
5	195	1.01	17.4
6	283	0.55	18.3
7	187	1.13	32.1
8	251	0.49	20.9
9	287	0.68	15.5

The applied force at break, tensile strength, and elongation at break results are given in *Table III*. According to the applied force at break results, sample 9 has the maximum value. After the calculations using the Taguchi method, the optimum parameters that result in maximum applied force at break was calculated as (3, 3, 1, 2 from *Table I*), which implies the sample made from process parameters of 12 rpm pump speed, 1.5 mm spinneret diameter, 1.0 draw ratio, and 40°C draw temperature is optimum. Since linear density values are not taken into account at the measurements of applied force at break, these results are expected, because the maximum applied force at break will be at the maximum thickness of the fiber with minimum draw ratio. Spinneret diameter is also at the maximum value to obtain the highest fiber denier. The expected result for applied force at break was calculated as 309+/-12cN. After the fiber with the process parameters of 3, 3, 1, and 2 from *Table I* was produced for the verification test, the applied force at break of the sample was measured as 318cN, which is in the tolerance gap of the calculated and expected values of applied force at the break.

The maximum tensile strength was found at the 7th sample, as shown in *Table III.* After the calculations using the Taguchi method, the optimum parameters that result in maximum tensile strength was calculated as (2, 1, 3, 2) sample, which implies the

sample made from process parameters of 8 rpm pump speed, 1 mm spinneret diameter, 2.0 draw ratio, and 40°C draw temperature was optimum. The result was expected because the maximum tensile strength will be achieved when the fiber is drawn and the molecules of the PVDF fibers are oriented. Temperatures around 40°C help the orientation of the molecules. 8 rpm pump speed with 1mm spinneret size resulted in less porosity. The expected result for maximum tensile strength was calculated as 1.18+/-0.06cN/tex. After the fiber with the process parameters of 2, 1, 3, 2 was produced for the verification test, the tensile strength of the sample was measured as 1.14cN/tex, which is in the tolerance gap of the calculated and expected values of tensile strength.

Minimum elongation at break was taken as the desired value for this research, because when the fiber reaches its maximum draw ratio, it will elongate less during the test. The main purpose of the production of these fibers was to have the best piezo properties. These properties will be the highest when the highest molecular orientation is reached.

The minimum elongation at break was found at the 3rd sample as shown in *Table III*. After the calculations using the Taguchi method, the optimum parameters that result in minimum elongation at break was calculated as (1, 3, 3, 1) sample, which implies the sample made from process parameters of 4 rpm pump speed, 1.5 mm spinneret diameter, 2.0 draw ratio, and 25°C draw temperature was optimum. The expected result for maximum tensile strength was calculated as 12.0+/-0.36%. After the fiber with the process parameters of 1, 3, 3, 1 was produced for the verification test, elongation of the sample was measured as 12.2%, which is in the tolerance gap of the calculated and expected values of elongation at break.

TABLE IV. S/N Ratio Values Calculated for Applied Force at Break, Tensile Strength and Elongation at Break of PVDF Fiber Samples.

Sample ID	S/N (Applied Force at Break)	S/N (Tensile Strength)	S/N (Elongation at Break)
1	43.02	-5.3	-25.36
2	44.76	-1.08	-27.34
3	44.79	-0.33	-22.15
4	44.62	-0.79	-28.07
5	45.97	0.28	-24.8
6	49.22	-4.99	-25.33
7	45.56	1.17	-30.13
8	48.15	-5.96	-26.45
9	49.35	-3.24	-23.97
Average	**46.16**	**-2.25**	**-5.95**

To calculate the S/N ratios using the Taguchi method, the order of experiments was obtained by inserting parameters into the columns of an orthogonal array, L_9 (3^4), chosen as the experimental plan given in *Table II*. But the order of experiments was made randomly to avoid noise sources, which if not considered initially, could take place during an experiment and affect the results in a negative way. The interactive effects of parameters were not taken into account in the theoretical analysis because preliminary tests showed that they could be neglected. S/N values calculated from Eq. (1) and Eq. (2), and average S/N effects obtained from three replications are shown in *Table IV.*

After the S/N ratio values for applied force at break, tensile strength, and elongation at break were found, the effect of process parameters on these fiber properties were calculated using the data shown in *Table IV*. Calculated values are the average values of three results of each parameter. For example, for the applied force at break analysis, samples that were produced at 4 rpm pump speeds are the sample 1, sample 2, and sample 3. The S/N ratio average for 4 rpm pump speed was found by taking the average of 43.02, 44.76, and 44.79. The result is 44.19, which is shown in *Figure 4.* Having these values shows the effects of each parameter used for production of PVDF fibers to the measured fiber properties. All the data are shown in *Figures 4, 5,* and *6*.

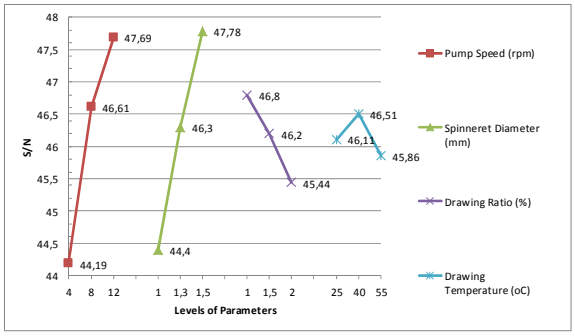

FIGURE 4. Average S/N Effects of wet spinning process parameters of PVDF fibers on applied force at break.

As shown in *Figure 4*, pump speed increased the applied force at break of the fibers. This was expected, because higher pump speeds result in more PVDF solution going out from the spinneret so the fiber produced from this polymer will be thicker. When the effect of spinneret diameters on applied force at break of the PVDF fibers is considered, the higher the spinneret diameter, the higher will be the applied force at break. This result was also expected, because higher spinneret diameter results in thicker fiber so the applied force at the break will be higher. At the higher draw ratios, applied force break decreases. This also shows that when the PVDF fiber is drawn at 40°C, rather than a decrease in porosity, a decrease in thickness of the fiber is seen, as shown in *Figure 3*. So drawing makes the fiber thinner and the applied force at break of the thinner fiber will be lower. 40°C-drawing temperature seems to be optimal for the drawing of PVDF fibers. It may be because of optimum molecular orientation and fiber solidification is at this temperature.

As shown in *Figure 5*, 8 rpm pump speed results in maximum tensile strength of PVDF fibers. Spinneret diameter affects the tensile strength negatively because higher spinneret diameter at the same feeding speed results in higher diameter of fiber with higher porosity in the fiber. The most effective wet spinning process parameter for the tensile strength is the draw ratio. As expected, results show that maximum tensile strength is achieved at the highest draw ratio because higher draw ratio of wet spinning decreases the porosity and orients the molecules in fiber.

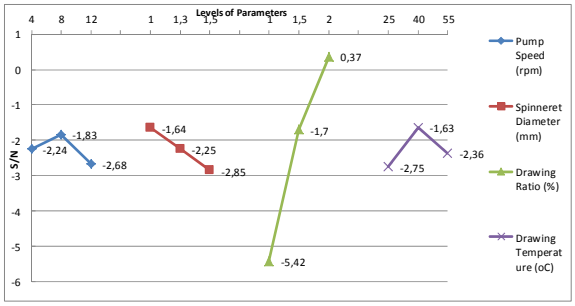

FIGURE 5. Average S/N Effects of wet spinning process parameters of PVDF fibers on Tensile Strength.

Figure 5 also shows the effect of draw temperature of wet spinning on tensile strength of PVDF fibers. A draw temperature of 40°C results in the maximum tensile strength of PVDF fiber. Higher draw temperatures in wet spinning may increase the solidification time of the fiber. So fiber may not have enough time in the bath to get solidified. On the contrary, higher drawing temperatures increase the molecular energy in the fiber so the molecules move much easier and molecular orientation of the fiber increases with one-axial drawing. Therefore, 40°C drawing temperature results in the highest tensile strength in the fiber.

As shown in *Figure 6*, the elongation at break will decrease with slower pump speed and higher spinneret diameter. This decrease may be because of more crystallinity in the fiber when higher diameter of the spinneret and lower pump speeds are used. Minimum elongation is reached when the fiber is drawn with 2.0 draw ratio and at a draw temperature as 25°C. The results were expected, because higher drawing ratio will draw the fiber more and the elongation at break will be less. Also molecules in the fiber do not have enough energy to move against each other at cooler temperatures around 25°C. Higher temperatures would make the molecules more energetic so they could move much easier.

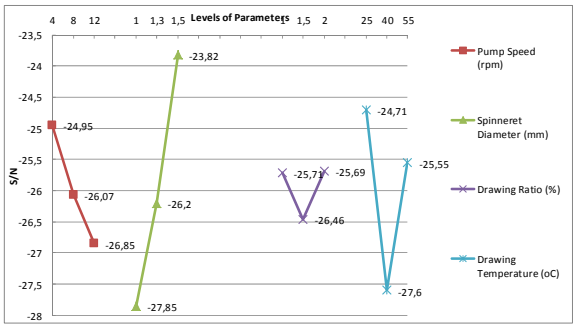

FIGURE 6. Average S/N Effects of wet spinning process parameters of PVDF fibers on elongation at break.

CONCLUSION

In conclusion, the optimization of wet spinning parameters to produce PVDF fibers to the maximum applied force at break, maximum tensile strength, and minimum elongation at break was investigated using the Taguchi method. The optimum wet spinning parameters to produce PVDF fibers at the highest strength and applied force, and at the lowest elongation at break were determined.

The maximum applied force at break was achieved for the PVDF fiber made from the process parameters of 12 rpm pump speed, 1.5 mm spinneret diameter, 1.0 draw ratio, and 40°C draw temperature. The maximum tensile strength was achieved for the PVDF fiber made from the process parameters of 8 rpm pump speed, 1mm spinneret diameter, 2.0 draw ratio, and 40°C draw temperature. The minimum elongation at break was achieved at 4 rpm pump speed, 1.5 mm spinneret diameter, 2.0 draw ratio, and 25°C draw temperature. These process parameters could be used for the further production of PVDF fibers.

When the average S/N effects of wet spinning process parameters of PVDF fibers were investigated, 8 rpm pump speed resulted in maximum tensile strength of PVDF fibers; drawing temperature of 40°C resulted in the maximum tensile strength of PVDF fiber; and higher spinneret diameter at the same feeding speed resulted in higher diameter of fiber with higher porosity in the fiber.

In addition to above results, the Taguchi method was found to be reliable for studying the wet spinning of PVDF fibers.

ACKNOWLEDGMENT

The author wishes to thank Dr. Sinan HINISLIOGLU for his help and efforts completing this research.

REFERENCES

[1] S. Choi, Z. Jiang, A novel wearable sensor device with conductive fabric and PVDF film for monitoring cardiorespiratory signals, Sens. Actuators A: Phys. 128 (2006) 317–326.

[2] L. Yang, C. Hsu, J. Ho, C. Feng, Flapping wings with PVDF sensors to modify the aerodynamic forces of a micro aerial vehicle, Sens. Actuators A: Phys. 139 (2007) 95–103.

[3] N. Snis *et al.*, Monolithic fabrication of multilayer P(VDF-TrFE) cantilevers, Sens. Actuators A: Phys. 144 (2008) 314–320.

[4] N.S. Shenck, J.A. Paradiso, Energy scavenging with shoe-mounted piezo electrics, IEEE Micro. 21 (2001) 30–42.

[5] J. Granstorm *et al.*, Energy harvesting from a back pack instrumented with piezoelectric shoulder straps, Smart Mater.Struct. 16 (2007) 1810–1820.

[6] Dongliang Wang, K and W.K Teo, Preparation and characterization of polyvinylidene fluoride (PVDF) hollow fiber membranes, Journal of Membrane Science, Volume 163, Issue 2, pp. 211–220, 1999.

[7] S.P. Deshmukh, K. Li, Effect of ethanol composition in water coagulation bath on morphology of PVDF hollow fibre membranes, Journal of Membrane Science, Volume 150, Issue 1, pp. 75–85, 1998.

[8] Li-Yun Yu *et al.,* Preparation and characterization of PVDF–SiO_2 composite hollow fiber UF membrane by sol–gel method, Journal of Membrane Science, Volume 337, Issues 1–2, 15, pp. 257–265, 2009.

[9] Koseki Yu *et al.,* Crystalline structure and molecular mobility of PVDF chains in PVDF/PMMA blend films analyzed by solid-state ^{19}F MAS NMR spectroscopy, Polymer Journal, 44, 757-763, (2002).

[10] http://www.tikp.co.uk/knowledge/technology/fibre-and-filament-production/wet-spinning/, 08/13/2013.

[11] Haagensen D., Development of a piezoelectric polymer fibre, MS Thesis, *Dep. of Materials and Manufacturing Technology,* Chalmers University of Technology, Göteborg, Sweden, 2010.

[12] Abid Omar, Processing, morphology and product parameters of PVDF filaments for biomedical applications, PhD Thesis, Institut für Textiltechnik der RWTH Aachen, 2008.

[13] Lau JH and Chang C. Taguchi design of experiment for wafer bumping by stencil printing. IEEE Trans Electron Pack Manuf 2000; 23: 219-225.

[14] Jaisingh A. *et al.*, Sensitivity analysis of a deep drawing process for miniaturized products. J Mater Process Technology, 2004; 147: 321-327.

[15] Yang WH and Tarng YS. Design optimization of cutting parameters for turning operations based on the Taguchi method. J Mater Process Technology, 1998; 84: 122-12.

[16] Kwok Leung T., An overview of Taguchi Method and newly developed statistical methods for robust design, IIE Transactions, 24, 44-57 (1992).
[17] Engin A.B., Color removal from textile dyebath effluents in a zeolite fixed bed reactor: Determination of optimum process conditions using Taguchi method, Journal of Hazardous Materials, 159, 348-353 (2008).
[18] Zeydan M., Modeling the woven fabric strength using artificial neural network and Taguchi methodologies, International Journal of Clothing Science and Technology, 20, 104-118, (2008).
[19] Hinislioglu, S. and Bark, Ü, O., "Optimization of Early Flexural Strength of Pavement Concrete with Silica Fume and Fly Ash by Taguchi Method" Civil Engineering and Environmental Systems, 21, No. 2, 79-90, 2004.
[20] Gunay B and Hinislioglu S, Traffic microsimulation scenario tests by the Taguchi method, Proceedings of the ICE - Transport, Volume 164, Issue 1, January 2011 , pages 33 –42 , ISSN: 0965-092X, E-ISSN: 1751-7710.

AUTHORS' ADDRESSES

Mevlut Tascan, PhD
Zirve Üniversitesi
Kızılhisar Kampüsü
Gaziantep 27260
TURKEY